Mitochondrial protein prohibitin enhances learning memory recovery in mice following intracerebral hemorrhage via CAMKII/CRMP Signaling Pathway.

Tianlin Jiang[1], Jiahua Wang[2], Yanli Wang[3], Jiawei Zhou[1], Xiaohong Wang[4, 5, 6*], Jun Xu[3*]

[1]Medical College, Yangzhou University, China, [2]Affiliated Hospital of Yangzhou University, China, [3]Beijing Tiantan Hospital, Capital Medical University, China, [4]Institute of Translational Medicine, Yangzhou University, China, [5]Jiangsu Key Laboratory of Experimental & Translational Non-coding RNA Research,, China, [6]Jiangsu Co-innovation Center for Prevention and Control of Important Animal Infectious Diseases and Zoonoses, College of Veterinary Medicine, Yangzhou University, China

Submitted to Journal:
Frontiers in Neuroscience

Specialty Section:
Translational Neuroscience

Article type:
Original Research Article

Manuscript ID:
1017193

Received on:
11 Aug 2022

Journal website link:
www.frontiersin.org

Conflict of interest statement

The authors declare that the research was conducted in the absence of any commercial or financial relationships that could be construed as a potential conflict of interest

Author contribution statement

XW and JX conceived and designed the study. TJ and JW performed animal experiments. YW and JW performed the behavioral assessments. TJ and JZ performed the Western Blot and Immunostaining analysis. YW analysed GSEA. TJ contributed generation of the manuscript. All authors contributed to the editing of the manuscript.

Keywords

Prohibitin (PHB), intracerbral hemorrhage, CaMK II, mitochondrial, Memory, Cognition, CRMP

Abstract

Word count: 242

Aim: Prohibitin (PHB) is a mitochondrial inner membrane protein with proven neuroprotective activities, antioxidant, and apoptosis-reducing effects. This study aimed to explore the role of PHB on pathological symptoms, behavioral deficits, and cognitive impairment in a collagenase-IV-induced intracerebral hemorrhage (ICH) murine model.

Methods: Mice received collagenase IV injection were pretreated with PHB or saline 21 days before modeling. The role of PHB on memory and learning ability was monitored by Morris water maze, Y-maze, rotarod test, social test, startle test, and nest building test. The effect of PHB on depress-like symptoms was examined by forced swimming test, tail suspension test, and sucrose preference test. Subsequently, mice samples were detected by immunohistology, western blotting, Perls staining, Nissl staining, and gene sequence.

Results: Collagenase IV significantly induced behavioral deficits, brain edema, cognitive impairment, and depress-like symptoms. PHB overexpression can effectively alleviate memory, learning, and motor deficits in ICH mice. PHB markedly inhibited the number of terminal deoxynucleotidyl transferase dUTP nick-end labeling (TUNEL)-positive cells and protein levels of Iba-1, GFAP, IL-1β in the perihematomal region in ICH mice. PHB overexpression also remarkably promoted the production of neurologin1 (NLGL1) and postsynaptic density 95 (PSD95), and upregulated levels of Ca2+-calmodulin-dependent kinase II (CAMK2) and Collapsin Response Mediator Protein-1 (CRMP1) proteins.

Conclusion: PHB overexpression can effectively alleviate the neurological deficits and neurodegeneration around the hematoma region. It may play a protective role by upregulating the expression of NLGL1 and PSD95 and promoting the expression of CAMK2 and CRMP1.

Contribution to the field

Prohibitin (PHB) is a mitochondrial inner membrane protein with many roles. Its roles in central nervous system diseases have been much studied. PHB mainly plays an anti-inflammatory, anti-apoptotic, maintenance of mitochondrial morphology and metabolism, and plays a role in the nervous system in protecting synaptic plasticity. This article reveals for the first time the alleviating effects of PHB on memory deficits and cognitive impairment after intracerebral haemorrhage (ICH), and proposes that PHB overexpression reduced cognitive deficits by upregulating expression of PSD95 and NLGL1, and activation of CaMKII/CRMP signalling in the perihematomal region of ICH mice.

Ethics statements

Studies involving animal subjects

Generated Statement: The animal study was reviewed and approved by Animal Ethics Committee of Yangzhou University.

Studies involving human subjects

Generated Statement: No human studies are presented in this manuscript.

Inclusion of identifiable human data

Generated Statement: No potentially identifiable human images or data is presented in this study.

Data availability statement

Generated Statement: The datasets presented in this study can be found in online repositories. The names of the repository/repositories and accession number(s) can be found in the article/supplementary material.

Title page

The title of the article：

Mitochondrial protein prohibitin enhances learning memory recovery in mice following intracerebral hemorrhage via CAMKII/CRMP Signaling Pathway.

The authors' names

Tianlin Jiang[†1], Jiahua Wang[†2], Yanli Wang[3], Jiawei Zhou[1,4,5], Xiaohong Wang*[1,4,5], Jun Xu*[3]

[†]stands for Equal contribution and first authorship

*stands for joint corresponding author

The complete affiliations of all authors

1. Institute of Translational Medicine, Medical College, Yangzhou University, Yangzhou, 225009, China
2. Department of Anesthesia, Affiliated Hospital of Yangzhou University, Yangzhou 225001, China
3. Department of Neurology, Beijing Tiantan Hospital, Capital Medical University, Beijing, China
4. Jiangsu Key Laboratory of Experimental & Translational Non-coding RNA Research, Yangzhou University, YangZhou 225001, China
5. Jiangsu Co-innovation Center for Prevention and Control of Important Animal Infectious Diseases and Zoonoses, Yangzhou, 225009

The name, postal and e-mail addresses of the corresponding author

Xiaohong Wang, Institute of Translational Medicine, Medical College, Yangzhou University, Yangzhou, 225009, China. Email: wxhong@yzu.edu.cn

Jun Xu, Department of Neurology, Beijing Tiantan Hospital, Capital Medical University, Beijing Tiantan Hospital, Capital Medical University,
No.119 South 4th Ring West Rd, Fengtai District, Beijing 100070, China. Email: neurojun@126.com

Abstract

Aim: Prohibitin (PHB) is a mitochondrial inner membrane protein with proven neuroprotective activities, antioxidant, and apoptosis-reducing effects. This study aimed to explore the role of PHB on pathological symptoms, behavioral deficits, and cognitive impairment in a collagenase-IV-induced intracerebral hemorrhage (ICH) murine model.

Methods: Mice received collagenase IV injection were pretreated with PHB or saline 21 days before modeling. The role of PHB on memory and learning ability was monitored by Morris water maze, Y-maze, rotarod test, social test, startle test, and nest building test. The effect of PHB on depress-like symptoms was examined by forced swimming test, tail suspension test, and sucrose preference test. Subsequently, mice samples were detected by immunohistology, western blotting, Perls staining, Nissl staining, and gene sequence.

Results: Collagenase IV significantly induced behavioral deficits, brain edema, cognitive impairment, and depress-like symptoms. PHB overexpression can effectively alleviate memory, learning, and motor deficits in ICH mice. PHB markedly inhibited the number of terminal deoxynucleotidyl transferase dUTP nick-end labeling (TUNEL)-positive cells and protein levels of Iba-1, GFAP, IL-1β in the perihematomal region in ICH mice. PHB overexpression also remarkably promoted the production of neurologin1 (NLGL1) and postsynaptic density 95 (PSD95), and upregulated levels of Ca2+-calmodulin-dependent kinase II (CAMK2) and Collapsin Response Mediator Protein-1 (CRMP1) proteins.

Conclusion: PHB overexpression can effectively alleviate the neurological deficits and neurodegeneration around the hematoma region. It may play a protective role by upregulating the expression of NLGL1 and PSD95 and promoting the expression of CAMK2 and CRMP1.

Introduction

ICH is a fatal central nervous system disease that now threatens human health (Zhang et al., 2016). ICH is characterized by inflammation, apoptosis, mitochondrial dysfunction, and cognitive impairment (Wei et al., 2022). Among them, decreased expression of memory and cognitive-related proteins are important mechanisms influencing the development of ICH (Wei et al., 2022).

Prohibitin (PHB) is a mitochondrial inner membrane protein, the main members of which are PHB1 and PHB2, which form a ring-like structure in the mitochondria and play a role in stabilizing mitochondrial metabolism and structure (MacArthur et al., 2019). In neuronal injury caused by neurological diseases, PHB plays important role in maintaining mitochondrial homeostasis, promoting gene transcription, and preventing cellular senescence (Osman et al., 2009).

Lachén-Montes et al. discovered that increased levels of PHB1 dephosphorylation in the olfactory bulb led to a decrease in the activation of several transcription factors, thereby affecting the development of Alzheimer's disease (AD) (Lachen-Montes et al., 2017). Qu et al. found that PHB S-nitrosylation was increased in neurons in the CA1 region of the hippocampus in cerebral ischemia, protecting neuron activity (Qu et al., 2020). Zhou et al. found that PHB overexpression enhances binding to NDUFS3 and protects against MPTP-induced neurotoxicity of SY5Y cells (Zhou et al., 2012). Borgmann-Winter et al. found that PHB is a synaptic protein that is present in spine synapses and colocalizes with the presynaptic proteins bassoon and ProSAP2/SHANK3 (Borgmann-Winter et al., 2020).

Many published experiments on PHB function in neurological diseases were performed in Parkinson disease and cerebral ischemia. However, the current study detected the role of PHB in ICH mouse model. In this study, we found that PHB overexpression ameliorates cognitive impairment caused by neuronal damage, via assays like the Morris water maze, Y-maze, and forced swimming test. To examine the role of PHB at the protein level, we performed gene array and Gene Set Enrichment Analysis (GSEA) analysis on mice samples and found that the most relevant pathways to the effects of PHB were the CAMKII pathway and the calcium pathway. Among them, 1 protein that improved cognition and 3 proteins that improved memory were verified by western blot. We hypothesized that PHB could effectively upregulate the expression of PSD95, NLGL1, CAMKII, and CRMP1, reducing cognitive impairment and improving the prognosis of ICH.

Materials and Methods

2.1 Experimental Animals

Adult C57/BL6 mice (male, aged 8 to 10 weeks) were procured from Yangzhou University's Comparative Medical Center. All of the mice were kept in places where they could eat and drink freely and where the light and dark cycled every 12 hours. All studies and procedures were approved by Yangzhou University's Institutional Animal Care and Use Committee and Animal Ethics Committee [SYXK (Su) IACUC 2017-0045].

2.2 ICH mouse model

Anesthesia was induced (5% in 100% O_2) and maintained with isoflurane. Mice were mounted on a stereotaxic frame to create the ICH model. The right caudate putamen was injected with bacterial collagenase IV solution (0.04 U) from Sigma-Aldrich Co., USA, dissolved in 0.2 L of saline. Collagenase IV was injected through ML=+3.7 mm, AP=+0.2 mm, and DV=-3.8mm to the bregma. Retract the needle with the speed of 1 mm per minute after another 5 minutes to cease reflux. Sham animals underwent a similar operation, with the exception that the same amount of phosphate buffered saline was injected into them instead.

2.3 PHB-AAV injection

To look into the function of PHB in ICH rodents, we injected PHB overexpression particles into the mice striatum 21 days before injecting collagenase IV, using PHB green particles originating from Hanbo Biotechnology (Shanghai, China). After inhalation anesthesia was given to each animal, and they were all put on a stereotaxic device. The green fluorescent protein-marked PHB overexpression AAV particles (2.1 10^7 TU/mL) were injected into the right striatum of the test animals. The injection coordinates were 0.8 mm laterally, 1.8 mm anteriorly, and reaching a depth of 3.0 mm to the bregma. Before taking the needle out of the brain, it was left there for five minutes to give the solution time to spread.

2.4 Laser speckle contrast imaging (LSCI)

All mice underwent LSCI (R500, RWD Life Science Co., LTD, China). Imaging was taken 1day prior to ICH (baseline imaging), then respectively at 24 h, 48 h, and 72h after ICH. Anesthesia was induced and maintained with isoflurane as discussed above, while animals were placed in a stereotaxic frame on a 37°C heat blanket. LSCI runs for 3 minutes at 19 fps (20 ms per frame, 10-s intervals). LSCI images were analyzed by moorFLPI2 Full-Field Laser Perfusion Imager Review v5.0 software.

2.5 Neurobehavioral Function Test

By using the forelimb placement test and corner test, neurobehavioral functions were evaluated. All of the behavioral evaluations took place between 9:00 and 11:00 am in a quiet room daily by two experimenters who are unaware of the tests.

Corner turn test

The animals (n=9) in each group were placed in a 30°corner, and they can exit by turning to the left or the right. We only kept track of the turnings that had full rearing along either wall. Mice have a propensity to turn to the injured side immediately following ICH operation (Li et al., 2019). At intervals of one minute, the test was run ten times, and the right turns percentage of each group was recorded.

Forelimb placement test

The animals (n = 9 in each group) were placed parallel to a table and progressively raised and lowered, allowing their vibrissae to brush the table's surface. By counting the number of correct forelimb placements over the course of 10 successive trials, refractory placements of the defective (left) forelimb were assessed.

Modified neurological severity score (mNSS)

To assess the functional consequences of the nervous system, mNSS was calculated. The scale ranged from 0 to 10 points (normal to severe). The mNSS consists of motor (muscle status and aberrant movement) and sensor (optical, tactile, and proprioceptive) assessments, as well as reflex reactions and balancing tests. If mice fail to perform the test or do not exhibit the predicted reaction, one point is granted; hence, the greater the score, the more extreme the injury.

2.6 Brain water content

Brain water content was detected three days following the collagenase IV injection. Brains were dissected and divided into 2 cerebral hemispheres (n=9 per group). Utilize an electric analytic balance to determine each hemisphere's wet weight. Brain tissues were dried at 120°C for 24 hours until no weight changed, then the dry weight was determined. Brain water content = (wet weight - dry weight)/wet weight 100 percent.

2.7 Nissl Assay and Immunohistochemical Staining

3 days after the operation, animals were transcardially perfused with normal saline and 4% paraformaldehyde. Brains were dissected and dehydrated, and 4um thick coronal sections were collected using a microtome. Sections were de-waxed and hydrated through xylene and graded ethanol. Nissl assay was carried out using a cresyl violet staining kit (Solarbio, China).

For the immunohistochemical staining, sections were heated in sodium citrate buffer for 10 minutes. Sections were incubated in 0.3% Triton X-100 and 3% H_2O_2 in methanol for 10 min separately, blocked with 5% normal goat serum, and were incubated with the primary antibodies anti-Iba-1(ET1705)(1:200, Huabio, China), anti-IL-1β(sc-52012)(1:200, Santa Cruz Biotechnology) and anti-GFAP (EM140707) (1:200, Huabio, China) at 4 ℃ overnight, followed by HRP-conjugated goat anti-Rabbit IgG H&L (ab6721) (1:200; Abcam plc, Cambridge, UK). Sections were stained in DAB (Zymed Laboratories Inc., San Francisco, CA, USA). The images were collected using a microscope (Axioplan 2, Zeiss, Oberkochen).

For the immunofluorescence staining, brain sections were incubated with rabbit anti-SYP (ET1606) (1:200, Huabio, China) overnight at 4 ℃. Then slices were incubated with AlexaFluor594-conjugated secondary antibodies (ab150080) (goat anti-rabbit, 1:200, Abcam plc, Cambridge, UK) for 1 h at room temperature. The slices were incubated with DAPI for 5 min. The expression of SYP in neurons was collected under a fluorescence microscope using Image-Pro Plus 6.0 (Media Cybernetics, Silver Spring, MD, USA).

2.8 TUNEL Staining

TUNEL assay was used to determine neuron death in separate groups of mice (n=9) on day 3 following ICH surgery. The sections were rinsed with PBS, then treated with a protease K solution containing 20 g/ml. The slices of the brain were then cleaned and incubated with the TUNEL reaction solution. Then, brain sections were stained for 5

minutes with DAPI. Under a fluorescent microscope, TUNEL-positive cells were detected and quantified.

2.9 Perls Staining

Slices were submerged in distilled water for three minutes prior to incubation in Perls solution (5% potassium ferrocyanide [SigmaAldrich, USA] in 5% HCL) for 30 min, followed by rinsing in PBS. Then inhibited endogenous peroxidase activity with 0.3% H_2O_2. Signals were created using 3,3diaminobenzidine (DAB; Vector Laboratories, USA) for 2 minutes, and hematoxylin (SigmaAldrich, USA) was utilized as a counterstain. As previously mentioned, an experimenter who was blind to the group identities counted the cells. Examining four randomly selected microscopical sections at a magnification of 200, the number of iron-positive cells in the contusion region was assessed.

2.10 Assessment of cognitive function impairment

Rotarod Test

As described previously, all mice (n=9 per group) were trained by an experimenter strange to the experiment, at the speed of 20 rpm for 5 minutes, 3 times/day for successive 4 days before ICH induction(Pan et al., 2018). The mice that fell off the rod were put back with minimal disturbance. After ICH operation, selected mice were put into 3 trials at the speed of 40 rpm, with a 5-minute rest between each trial. The duration to fall of each trial was recorded. The mice staying on the stick for more than 300s were removed and the latency to fall was recorded as 300s.

Morris Water Maze (MWM)

Each trial was conducted in an environment suitable for behavioral testing. The water labyrinth apparatus consisted of a round tank (diameter:120 cm) containing water with about 20-22°C, and an exit platform (PVC, diameter: 10 cm) buried 0.8 cm below water. The water was opaque to conceal the hidden platform. Essentially, the tank was divided into four equal quadrants (north, east, south, and west). All spatial trial days have consisted of 4 trials, with random start positions. The mice were given 60 seconds to locate the platform before being allowed to remain on it for 15 seconds. If the mouse did not find the platform within 60 seconds, it was guided there and remained for 15 seconds. Then, on day six, the probing test was conducted, with the pool's hidden platform removed. In this method, mice were given 30 seconds to find the pool. To determine the long-term effects of PHB, the next phase of the water maze was initiated 21 days after ICH. Behavioral information on animals was gathered using a computerized video tracking system (ANY-maze 6.0, Stoelting, Co., Wood Dale, IL, United States). During the period of swimming, all mice save the one being tested were housed in heated cages. Except for the relocation of the platform to the southwest region and the establishment of a new starting point, the experimental technique was identical to what had been stated previously.

Y -Maze

The Y-maze apparatus was utilized to evaluate working memory and discovery behavior (40 cm in length, 3 cm in bottom width, 13 cm in upper width, 15 cm in height) (Cleal et al., 2021). Use an animal-safe disinfectant to sanitize the Y-maze, and then use paper towels

to remove all remnants of the disinfectant. Ensure the maze is devoid of dampness. Each rodent was placed in the center of the area. During the first ten minutes, the number of alterations and entries into the new arms were recorded. Working memory was calculated as the ratio of correct adjustments to the total number of new arm entries.

Social test

Before testing, mice were exposed to the testing environment for at least one hour. The 3-chamber sociability and social novelty tests were administered as previously reported, with a few minor adjustments (Bertoni et al., 2021). The testing apparatus consisted of a translucent Plexiglas box (60cm W 40cm D 20cm H) with 3 chambers separated by two transparent partitions with square-shaped opening doors (8 x 6 cm). A test mouse was given 10 minutes to explore the entire habitat with the doors open in order to acclimate. The inanimate object stimulus (E) was a 10-cm diameter cylindrical wire cage with no object inside, whereas the social stimulus (S) was a round wire cage with a new mouse inside (S1). A test mouse was placed in the center with doors shut, while E and S1 were positioned in the upper corners of each side chamber. When the doors were opened, a video camera was used to capture the mice's activity for 10 minutes to assess their friendliness (S1 vs E). A test mouse was allowed to freely explore both the S1 (familiar) and S2 (unfamiliar) mice for 10 minutes during the social novelty test. The arena and cylindrical wire cages were cleaned between each subject with 70 percent ethanol and dry paper. Carefully selected mice of the same gender and age were never exposed to the test animal before testing began. Before testing, mice were acclimated to the wire cage for 10 minutes. Measure the time spent sniffing each target.

Forced Swimming Test (FST)

To evaluate behavioral discomfort in the FST, mice were allowed to swim in a 2L glass beaker with 75% of its capacity of water. Before each experiment, the beaker was cleaned thoroughly. The water temperature was regulated between 21 and 25 degrees Celsius. The mouse was placed in the container's center by gently gripping its tail. Five minutes of their conduct were captured on film, and the full five minutes were analyzed. The FST procedure was derived from earlier research; 6-minute FST protocols with the first two minutes deleted have also been used. This study's technique selection was based on a previously specified methodology for a similar chronic stress paradigm. Every effort was made to reduce the effect of light reflected from the surface of the water. 100-120 lx of light intensity were positioned at the level of the beakers 10 feet above the behavioral setup. A white, non-reflective covering with a matte finish was placed beneath the beakers to decrease glare. The camera was placed horizontally three feet away from the beakers and at water level. The camera and beakers stayed in the same position across multiple days of video recordings.

After the test, the mice were dried, placed in a warm (30-33°C) container for 20 minutes, and then returned to their home cage. The mouse was considered immobile for the purposes of manual analysis when it floated passively and could only make movements to keep its head above water. Compared to overall time, the amount of time spent in inactivity was logged (100s).

Tail suspension test (TST)

During the TST, mice were hung for five minutes by their tails. As previously described,

C57BL6 mice exhibit significant tail climbing behavior; therefore, we passed the tail through a lightweight (0.5 g) plastic tube to prevent tail climbing. The camera position and lighting settings paralleled those of FST. After tests, mice were placed in a holding cage until all mice in their home cage were tested. The duration of immobility was recorded and compared to the total time (150s).

Nest building test

Before surgery, each mouse was freely assigned to an experimental group. All analyses were conducted without the use of eyesight. Throughout the tests, mice were kept in individual cages with woodchip bedding and had free access to food and drink. In the "home" cage, mice engaged in nest-building behavior organically and independently. Normal mice can build a nest in less than 10 minutes. This research employed a 5 cm square of compressed cotton batting as the nestles. The nestle was made from pulped virgin cotton fiber, was sterilized throughout production, and was packaged in a sanitary manner. Nestles do not degrade during storage. There were only 2.5 g of nestlings used. The nests were assessed according to Torre's 5-point scale from1 to 5 as follows: 1 = not noticeably touched, 2 = partially torn up, 3 = mostly shredded but often no identifiable site, 4 = identifiable but flat, and 5 = perfect or nearby.

Sucrose preference test

For fifteen hours, remove all food and drink containers from the cages. For nighttime measurements on the sixth day, 7 a.m. to 10 p.m. are used. For daytime measurements, from 6 p.m. on the first day until 9 a.m. on the seventh, inclusive. Verify that the device has been prepared as indicated throughout this time. Turn on the electricity to the SPT electronic equipment on Day 2. Immediately after deprivation at 9:00 a.m., bring the home cages to the test room and randomly arrange mice from their home cages into apparatus chambers. Click the start button to initiate data collecting for the experiment. After a predetermined length of detection, the software-MDA would automatically pause. Return the mice to their original cages and provide them unrestricted access to food and water. Click "analysis" on the software-MDA; the period can be chosen to 30 minutes, 60 minutes, or a different number; then export the trial results to analyze the data, which includes the consumption periods and total time of sucrose water or plain water. Use the equations below to determine sucrose preference: preference = (sucrose consumption duration / total consumption duration) 100%. Total consumption time equals the sum of sugar and regular water drinking durations. Cleanse the laboratory carefully. Finally, use 70% ethanol to eradicate odors.

Startle Test

We used the fear conditioning paradigm (XRXC404, Softmaze Information Technology Co. Ltd., Shanghai, China; 30 cm in length, 26 cm broad, 22 cm high) to assess hippocampus-related learning and memory. On the day of the acquisition, mice were familiarized for 2 min, given four 2-s, 0.4 mA foot shocks spaced 2 min apart, and then put back in cages for a further 2 min. The day 2 experiment was conducted the following day in the identical chamber for 6 minutes by assessing the period of freezing as a measure of fear memory.

2.11 Western Blotting Analysis

The brain tissues surrounding the hematoma of each group were collected and homogenized in ice-cold lysis buffer. Brain extracts run on 8%, 10%, or 12% SDS-PAGE and were transferred onto nitrocellulose membranes (Millipore, Massachusetts, USA). The membranes were blocked with 5%BSA and were incubated with primary antibodies against CRMP1(Huabio, China, Lot: ET7106-86, 1:1000 dilution), β-actin (1:2000) (Abcam plc, Cambridge, UK), BDNF(Huabio, China, Lot: ER130915, 1:1000 dilution), CaMKII(Huabio, China, Lot: ET1608-47, 1:1000 dilution), PSD95(Huabio, China, Lot: ET1602-20, 1:1000 dilution) and NLGL1(Proteintech, China, Lot: 66964-Ig, 1:1000 dilution) at 4℃ overnight. The membranes were then washed and incubated with secondary antibody for 1h at room temperature. The protein bands were detected by super enhanced chemiluminescence and the density of bands was analyzed by the ImageJ software.

2.12 RNA sequencing

An RNeasy micro kit purified RNA (QIAGEN, Hilden, Germany). Following the manufacturer's instructions, a library for next-generation sequencing was created using the TruSeq RNA Sample Preparation Kit V2 (Illumina, San Diego, CA). Amplified cDNA was ligated with sequencing adapters and barcodes to create sequencing-ready cDNA libraries. Shanghai Biotechnology Corporation (China) sequenced using Illumina's HiSeq 2500 platform.

Each sample's sequencing data were aligned to the reference genome. Four processes were used with default parameters to reconstruct transcripts, find novel transcripts, quantify transcripts, and normalize expression levels (FPKM, Fragments per Kilobase of transcript per Million mapped reads). R (3.2.1) and edgeR were used to find differentially expressed genes (DEGs). Fold change = Log2 (Experimental/Control group). In this study, DEGs had a |logFC| > 1 and a q-value 0.05. Using the ward technique for the euclidean distance matrix, DEGs were clustered hierarchically to depict expression patterns. Clustered gene expression profiles were shown by each group's mean log2(FPKM). Interproscan (v.5.8-49.0) and blast2go were used to annotate domains, gene families, and GO activities. Genes were mapped using KOBAS (v2.0)6 with default parameters. A hypergeometric distribution test identified GO functions and KEGG pathways whose DEGs were significantly enriched (q-value 0.05) relative to background expression genes. Enriched GO items and KEGG pathways were plotted with Python (v.2.7.5) and matplotlib (v.1.4.2).

2.12 Data Analysis

All outcomes were represented as the mean standard deviation (SD) of at least three independent, replicated studies. SPSS software was used to conduct statistical analyses utilizing a Student's t-test or one-way ANOVA or two-way ANOVA. P values less than 0.05 were deemed statistically significant.

Results

3.1 PHB significantly suppressed the neurological deficits and brain edema of ICH Mice

To investigate the impact of PHB on ICH, the neurological deficits and brain edema of

three groups were measured. The collagenase IV injection resulted in a hematoma, the PHB overexpression significantly suppressed hematoma volume (Fig.2B). To validate this, we measured the volume of the hematoma (Fig.2C, $^{***}p<0.001$ versus the sham group, $^{###}p<0.001$ versus the ICH group). For the impairment of the nervous system (motor, sensory, balance, and reflex functions) caused by ICH, we rated the 3 groups using the mNSS score. Our research found that the PHB overexpression group showed significantly less neurological impairment than the model group (Fig.2D, $^{***}p<0.001$ versus the sham group, $^{##}p<0.01$ versus the ICH group). Moreover, we detected brain edema to verify the PHB functions. Fig.2E reveals that, with PHB overexpression, brain water content is remarkably reduced compared with the ICH group ($^{***}p<0.001$ versus the sham group, $^{##}p<0.01$ versus the ICH group). In addition, we used the Corner Turn Test to evaluate the motor deficits of mice. In the control group, the probability of going left or right during cornering is random; nevertheless, mice with ICH preferentially turn to the non-damaged ipsilateral side. Fig.2F reveals that similar to the control group, mice in the PHB +ICH group showed less severe hemiparesis symptoms than mice in the ICH group($^{***}p<0.001$ versus the sham group, $^{#}p<0.05$ versus the ICH group). The forelimb placement test was used to examine the anterior and lateral limb positioning response and the function of abduction and adduction in mice. In the forelimb placement test, animals of the control group were able to position the ipsilateral forelimb on the table corner in response to tentacles. PHB overexpression group showed a higher rate of left paw placement compared with the ICH group (Fig.2G, $^{***}p<0.001$ versus the sham group, $^{##}p<0.01$ versus the ICH group). This suggests that PHB may effectively increase the sense-motor function of mice. Apoptosis was associated with the degeneration of neurons in mice (Fig2H-J, $^{***}p<0.001$ versus the sham group, $^{##}p<0.01$ versus the ICH group). Nissl staining revealed that the neurons in the hippocampal region of the sham group of mice had normal morphology, neat layout, and no apoptotic necrosis; however, the number of neurons in the hippocampal area of the ICH group was significantly reduced, with cytosolic swelling, nuclear consolidation, and disorderly arrangement. A limited number of apoptotic neurons were seen in the hippocampal of normal mice, but a substantial number of TUNEL-positive apoptotic neurons were observed in the hippocampal of model animals ($^{***}p<0.001$ versus the sham group, $^{##}p<0.01$ versus the ICH group). TUNEL-positive cells were dramatically decreased in the PHB overexpression group, demonstrating that PHB had a considerable inhibitory impact. This suggests that PHB overexpression can prevent apoptosis in hippocampus neuronal cells of ICH mice.

3.2 PHB protects cerebral blood volume during post-hemorrhagic stages

As depicted in Fig.3, intracerebral blood flow decreased in the PHB overexpression group after collagenase IV injection, whereas blood flow increased sharply in the ICH group; this difference persisted for 1 day after cerebral hemorrhage, suggesting that PHB can reduce cerebral hemorrhage by decreasing intracerebral blood flow during cerebral hemorrhage ($^{*}p<0.05$ versus the sham group , $^{#}p<0.05$ versus the ICH group). On the second day after cerebral hemorrhage, cerebral blood flow improved in the PHB overexpression group, but the ICH group showed signs of cerebral ischemia, leading to an ongoing increase in intracerebral blood flow($^{*}p<0.05$ versus the sham group, $^{#}p<0.05$ versus the ICH group).

On the third day, the cerebral blood flow of all groups gradually recovered. The detection of cerebral blood flow indicates that PHB has a dual protective effect on cerebral blood volume at all stages following cerebral hemorrhage, both in preventing excessive bleeding during cerebral hemorrhage and in rapidly restoring blood supply to the brain and reducing neurological damage.

3.3 PHB significantly lowers the inflammatory and ferroptosis response in ICH mouse brains.

The preceding studies demonstrate that PHB may play a regulatory role by decreasing the inflammatory and ferroptosis response in the ICH mouse brain. Fig. 4 demonstrates that the amount of GAFP, Iba-1, and IL-1β positive cells in the sham group was low, whereas the number of GFAP, Iba-1, and IL-1β positive neuronal cells in the hippocampal region of the ICH mice was significantly elevated, with GFAP and Iba-1-positive cells exhibiting amoeboid morphology, indicating the activation of astrocytes (***$p<0.001$ versus the sham group, $^{\#\#}p<0.01$ versus the ICH group). The amount of GFAP, Iba-1, and IL-1-positive neural cells in the hippocampus, as well as the number of activated astrocytes and microglia, decreased significantly in the PHB overexpression group($^{***}p<0.001$ versus the sham group, $^{\#\#}p<0.01$ versus the ICH group). Perl's staining, a test for iron death, found less ferroptosis and fewer bleeding cells in the normal group, but ferroptosis was pronounced in the brains of the model mice and the proportion of bleeding cells was low($^{***}p<0.001$ versus the sham group, $^{\#\#}p<0.01$ versus the ICH group). A considerable number of positive cells and a modest degree of ferroptosis were also related to excessive PHB expression in the brain($^{***}p<0.001$ versus the sham group, $^{\#\#}p<0.01$ versus the ICH group).

3.4 PHB ameliorates mice with ICH-related memory loss and depress-like symptoms

The period of operation for each behavioral trial is shown in Fig.5A. To examine the memory function of mice, we utilized the Morris water maze and found that the time to identify the platform and the number of times mice entered the platform were significantly reduced in ICH mice compared to the control group, whereas both values were comparable in PHB overexpression mice ($^{**}p<0.01$ versus the sham group, $^{***}p<0.001$ versus the sham group, $^{\#\#\#}p<0.001$ versus the ICH group). This indicates that PHB may sustain memory function in ICH-affected mice. Similarly, the Y-maze may be used to evaluate the memory capacity of mice. The memory performance of mice with PHB overexpression is superior to that of ICH mice, which is equivalent to that of the sham group, as measured by the number of correct turns and the number of steps in the Y-maze ($^{***}p<0.001$ versus the sham group, $^{\#}p< 0.05$ versus the ICH group). The startle test can be used to measure scene memory. By administering electric shocks to each of the three groups of mice, it was discovered that the level of rigidity in ICH mice was the lowest among the three groups, while the level of rigidity in the PHB group was in the middle, indicating that PHB could significantly enhance the memory function of brain hemorrhage to remember the frequency and intensity of electric shocks, which caused fear and rigidity ($^{**}p<0.01$ versus the sham group, $^{***}p<0.001$ versus the sham group, $^{\#}p< 0.05$ versus the ICH group, $^{\#\#}p<0.01$ versus the ICH group). The rotarod test may

determine mice's memory in addition to their balance and motor coordination. On the first day after cerebral hemorrhage, it is evident that the experimental results of both the PHB overexpression group and the model group were lower than those of the sham group, and that the mice in the PHB overexpression group gradually recovered to near normal levels over the next 2 to 4 days, whereas the damaged brain functions of the ICH group were irreparable(***p<0.001 versus the sham group, $^{\#\#}$p<0.01 versus the ICH group, $^{\#\#\#}$p<0.001 versus the ICH group). This shows that PHB has a role in supporting the balance and memory recovery of mice. The social test demonstrates that mice in the PHB overexpression group are less depressed than the ICH group(***p<0.001 versus the sham group, $^{\#\#\#}$p<0.001 versus the ICH group). And ICH mice were much more melancholy, displaying an unwillingness to explore new habitats and connect with strangers. This implies that PHB may alleviate autistic symptoms in ICH mice. The nest building test is an additional effective response to this issue. The mice in the PHB overexpression group had fewer autistic symptoms than those in the ICH group, but still moderate autistic signs relative to the control group (***p<0.001 versus the sham group, $^{\#\#}$p<0.01 versus the ICH group). This indicates that PHB may alleviate autism symptoms and improve mental difficulties in ICH mice.

3.5 PHB alleviates depression in ICH-affected rodents.

In assessments, PHB reduced depressive symptoms in mice after ICH, and we ran additional trials to corroborate this (Fig.6A). The forced swimming test on day 4 revealed that mice in the ICH group had the longest immobility time of the three groups, whereas mice in the PHB overexpression group had the shortest immobility time, indicating that their depressive symptoms were the mildest, suggesting that PHB can rapidly alleviate depressive symptoms in mice (***p<0.001 versus the sham group, $^{\#\#\#}$p<0.001 versus the ICH group). On day five, the tail suspension test indicated that the immobility duration of mice in the ICH group maintained the longest, while that of mice in the PHB overexpression group was shorter, although not as short as that of mice in the control group (***p<0.001 versus the sham group, $^{\#}$p< 0.05 versus the ICH group). On the sixth day, as measured by the sucrose preference test, this scenario became more obvious, the depressive symptoms of ICH mice were further intensified, while the treatment effect of mice in the PHB overexpression group tended to be stable and might alleviate depression (**p<0.01 versus the sham group, $^{\#}$p< 0.05 versus the ICH group).

3.6 PHB improves learning, memory, and cognitive deficits in ICH mice.

Given that PHB roles in memory loss and cognitive impairment have been discovered, we subsequently examined putative protein targets using gene sequence, GSEA analysis, and Western blotting. Pde10a and CAMKII gene expression, which are linked to learning and memory, were positively correlated with the PHB overexpression group (Fig.7A) and negatively correlated with the model group (Fig.7A), indicating that PHB expression may affect the enrichment of the two genes. Fig.7B indicates that the cognitive component of a biological process is the most important, followed by learning or memory. The synapses between neurons are the second most positively linked component of the cell. It is hypothesized that PHB influences synaptic connections to govern cognition, learning, and

memory. In the pathway enrichment analysis, it was determined that the calcium signaling pathway and the cAMP signaling pathway are positively associated with the therapeutic benefits of PHB. Fig.7C and 7D show a significant positive correlation between calcium channels and PHB overexpression, indicating that PHB may impact neuronal function by contributing to calcium channel activation. The positive connection between PHB expression and the CAMP signaling pathway implies that PHB may interact with CAMP to have a neuroprotective effect, indicating that PHB overexpression may enhance synaptic connectivity and affect synaptic function, hence affecting memory, cognition, and learning. Subsequently, we found that PHB overexpression improves LTP and, thus, protects against memory loss, which is consistent with the results of prior behavioral studies. In addition, we observed (Fig.7G) that the larger the expression of PHB in the serotonergic synapse, a crucial pathway linked with learning, memory, and cognition, the more prominent the serotonergic synapse. Moreover, Fig.7H demonstrates that axon guidance is positively correlated with PHB expression, showing that PHB is involved in memory protection.

Using western blotting, the quantities of proteins influencing learning, cognition, and memory were further investigated. As depicted in Fig.7I, the expression level of the synapse-related protein PSD95 was significantly decreased in the mice of the ICH group, whereas the level of PSD95 in the mice of the PHB overexpression group was comparable to that of the control group, indicating that PHB could mitigate the synaptic damage caused by ICH, thereby preventing memory deficits ($^{***}p<0.001$ versus the sham group, $^{###}p<0.001$ versus the ICH group). Moreover, cognition-related NLGL1 protein expression was lower in the ICH group and higher in the PHB overexpression group, showing that PHB offers cognitive protection through NLGL1 ($^{***}p<0.001$ versus the sham group, $^{###}p<0.001$ versus the ICH group). PHB could effectively improve the learning and memory performance of ICH mice, based on the production of the neurotrophic factor BDNF ($^{***}p<0.001$ versus the sham group, $^{##}p<0.01$ versus the ICH group). PHB is also involved in the CAMKII pathway, preventing memory loss as a result ($^{***}p<0.001$ versus the sham group, $^{###}p<0.001$ versus the ICH group). In addition, PHB overexpression reduces CRMP1 loss, preserving synaptic and memory function ($^{***}p<0.001$ versus the sham group, $^{##}p<0.01$ versus the ICH group). Additionally, SYP labeling can represent synaptic plasticity and the learning and memory function in animals. As seen in Fig.7J, the SYP-positive cells in the ICH group were significantly lower than in the sham group, indicating learning memory damage; the SYP-positive cells in the PHB overexpression group were significantly higher, indicating that PHB can promote multiple aspects of brain function including learning and memory in the brains of ICH mice ($^{***}p<0.001$ versus the sham group, $^{##}p<0.01$ versus the ICH group).

Discussion

PHB plays a crucial role in neurological diseases like Parkinson's disease (PD), AD, cerebral ischemia, and schizophrenia(Kurinami et al., 2014; Lachén-Montes et al., 2017; Borgmann-Winter et al., 2020; Yan et al., 2020). A low level of PHB results in mitochondrial abnormalities and aberrant mitochondrial hyperplasia, which in turn

increases ROS, accelerates neurodegeneration, and ultimately shortens lifetime (Yan et al., 2020). What's more, PHB overexpression protects SH-SY5Y cells against neurotoxicity induced by MPTP by enhancing and restoring the activity of NDUFS3, which encodes the 30 kDa subunit of mitochondrial complex I (Zhou et al., 2012). Lachén-Montes et al discovered that in the intermediate and later stages of Alzheimer's disease, PHB2 is significantly reduced whereas phosphorylated PHB1 are decreased. Additionally, PHB expression in olfactory is dysregulated in a variety of dementias. The overexpression of PHB2 in dementia and the deletion of PHB1 in frontotemporal lobar degeneration are additional indicators of a mitochondrial imbalance (Lachén-Montes et al., 2017). Kurinami et al. discovered that PHBs can protect hippocampus CA1 region neurons from ischemia and improve hippocampal dysfunction following ischemia. Overexpression of PHB in the mouse hippocampus reduced cytochrome c release and activated caspase-3. Thus, PHB can inhibit the generation of ROS following ischemia, prevent mitochondrial apoptosis, and mitigate cell death (Kurinami et al., 2014). Previous studies showed that PHB also functions in inhibiting inflammation and anti-apoptosis (Artal-Sanz and Tavernarakis, 2009; Jiang et al., 2022). This study also found that PHB plays an inflammatory inhibitory, anti-apoptotic role in the ICH mice model. Nissl staining and TUNEL assay showed a significant decrease in positive cells, suggesting that PHB plays a role in anti-apoptosis. A decrease in the expression of inflammation-related proteins, including Iba-1, GFAP, and IL-1β, could be found in the IHC results (Duan et al., 2021), suggesting a consistent role of PHB in suppressing the inflammatory response from ICH. These findings are all in line with previous research (Yang et al., 2015).

The visual manifestations after ICH include cerebral hematoma, increased brain water content, and hemiparesis (Hemphill et al., 2001). This study also shows that after ICH, cerebral blood flow increases for a short period and then decreases, and cerebral water content increases along with contralateral hemiparesis, which is reduced in the PHB overexpression group, suggesting a therapeutic effect of PHB in ICH.

Learning and memory deficit is representative in ICH patients. In the present study, ICH mice showed cognitive deficits as evidenced by obvious longer escape latency in the Morris water maze, obvious lower percent of correct turn in the Y-maze, obvious shorter duration on the bar in the rotarod test, reluctance to socialize with conspecifics in the social test, an inability of mice to recall pain from electric stimulation in the startle test due to poor memory and low scores in the nest building test. In addition, post-ICH can cause cognitive impairments such as depression and anxiety (Sawyer et al., 2021). This was also confirmed by the forced swimming test, the tail suspension test, and the sucrose preference test in this study. Furthermore, PHB overexpression was found to be effective in reducing symptoms of cognitive impairments and memory loss after ICH through the behavioral assessments described above. After PHB overexpression in the striatum in ICH mice, there was a noticeable improved in the number of crossing platforms and an obvious increase in the percentage of time in the target quadrant, compared to the ICH group. Also, PHB could significantly reverse the depress-like symptoms in ICH mice. Therefore, we preliminarily concluded that PHB is likely to improve learning and memory

deficits caused by ICH.

It is worth noting that inflammation, oxidative damage, and apoptosis have good correlations with learning and memory impairment in ICH patients (Bao et al., 2020; Schrag and Kirshner, 2020; Xue and Yong, 2020). Currently, studies have shown that medical treatments to inhibit inflammatory factors in the brain, such as microglia and invading peripheral leukocytes, could improve synaptic plasticity in animal models (Yang et al., 2015). Inflammation is primarily associated with the NF-κB signaling pathway, the PPARγ pathway, and other pathways (Jiang et al., 2017; Wu et al., 2018). mTOR, which is a downstream regulator of the PI3K/PKB pathway, plays an important role in Neurologic apoptosis (Feng and Huang, 2013). Connections of TLRs with pathogen-associated molecular patterns (PAMP) activate signaling via myeloid differentiation primary response-88 (MyD88) and induce the production of cytokines via excitation of the transcription factor nuclear factor kappa beta (NF-kB) (Li et al., 2011). In this study, immunohistological examination in ICH mice showed a great number of Iba-1 and GFAP positive cells, exhibiting amoeboid morphology, in the perihematomal area 3 days after the operation. Pretreatment of PHB could significantly inhibit the neuroinflammation in brain tissue induced by collagenase IV which fits well with our hypothesis.

PHB is also a synaptic protein that colocalizes with the presynaptic proteins bassoon and ProSAP2/SHANK3 at spine synapses (Borgmann-Winter et al., 2020). Synaptic plasticity is essential for the operation of hippocampal synapses, and plasticity in the hippocampus helps in the formation of new memories. Guoyot et al. demonstrated that treatment of aged mice with PDD005, which binds PHBs, increases the expression of SOX-2 and nestin by associating with PHBs in CNS cell membranes (Guyot et al., 2020). Few studies have been conducted on the relationship between PHB and synaptic plasticity, thus it will be beneficial to learn more about this area.

PSD95 and NLGL1 play a crucial role in learning and memory deficit and depression. To be more specific, phosphorylated PSD-95 promotes AMPAr stabilization at the synapse (Zanca et al., 2019). CaMKII contributes to synaptic transmission and is required for LTP maintenance (Tao et al., 2021). CRMP-1 is a specific signaling protein in brain and acts as a guidance factor in axon repellence (Luo et al., 2012). NLGL1 is another important protein involved in cognition. In ICH, the expression of the above proteins was significantly decreased, in line with previous studies (Luo et al., 2012; Wu et al., 2018; Zanca et al., 2019; Tao et al., 2021). In the PHB overexpression group, the expression of these proteins was increased, suggesting that this may be the mechanism of action involved in the alleviation of memory deficits and cognitive impairment with PHB treatment.

Conclusion

Our study has shown that overexpression of PHB suppressed collagenase IV-induced neurodegeneration, inflammation, and apoptosis in mice. PHB overexpression reduced cognitive impairment by upregulating the expression of PSD95 and NLGL1, and activation of CaMKII/CRMP signaling in perihematomal region of ICH mice. More efforts are needed

to uncover how PHB is associated with the above-mentioned biological processes.

Reference

Artal-Sanz, M., and Tavernarakis, N. (2009). Prohibitin and mitochondrial biology. *Trends In Endocrinology and Metabolism: TEM* 20(8)**,** 394-401. doi: 10.1016/j.tem.2009.04.004.

Bao, W.-D., Zhou, X.-T., Zhou, L.-T., Wang, F., Yin, X., Lu, Y., et al. (2020). Targeting miR-124/Ferroportin signaling ameliorated neuronal cell death through inhibiting apoptosis and ferroptosis in aged intracerebral hemorrhage murine model. *Aging Cell* 19(11)**,** e13235. doi: 10.1111/acel.13235.

Bertoni, A., Schaller, F., Tyzio, R., Gaillard, S., Santini, F., Xolin, M., et al. (2021). Oxytocin administration in neonates shapes hippocampal circuitry and restores social behavior in a mouse model of autism. *Molecular Psychiatry* 26(12)**,** 7582-7595. doi: 10.1038/s41380-021-01227-6.

Borgmann-Winter, K.E., Wang, K., Bandyopadhyay, S., Torshizi, A.D., Blair, I.A., and Hahn, C.-G. (2020). The proteome and its dynamics: A missing piece for integrative multi-omics in schizophrenia. *Schizophrenia Research* 217**,** 148-161. doi: 10.1016/j.schres.2019.07.025.

Cleal, M., Fontana, B.D., Ranson, D.C., McBride, S.D., Swinny, J.D., Redhead, E.S., et al. (2021). The Free-movement pattern Y-maze: A cross-species measure of working memory and executive function. *Behavior Research Methods* 53(2)**,** 536-557. doi: 10.3758/s13428-020-01452-x.

Duan, L., Zhang, Y., Yang, Y., Su, S., Zhou, L., Lo, P.-C., et al. (2021). Baicalin Inhibits Ferroptosis in Intracerebral Hemorrhage. *Frontiers In Pharmacology* 12**,** 629379. doi: 10.3389/fphar.2021.629379.

Feng, P., and Huang, C. (2013). Phospholipase D-mTOR signaling is compromised in a rat model of depression. *Journal of Psychiatric Research* 47(5)**,** 579-585. doi: 10.1016/j.jpsychires.2013.01.006.

Guyot, A.-C., Leuxe, C., Disdier, C., Oumata, N., Costa, N., Roux, G.L., et al. (2020). A Small Compound Targeting Prohibitin with Potential Interest for Cognitive Deficit Rescue in Aging mice and Tau Pathology Treatment. *Scientific Reports* 10(1)**,** 1143. doi: 10.1038/s41598-020-57560-3.

Hemphill, J.C., Bonovich, D.C., Besmertis, L., Manley, G.T., and Johnston, S.C. (2001). The ICH score: a simple, reliable grading scale for intracerebral hemorrhage. *Stroke* 32(4)**,** 891-897.

Jiang, T., Wang, J., Li, C., Cao, G., and Wang, X. (2022). Prohibitins: A Key Link between Mitochondria and Nervous System Diseases. *Oxidative Medicine and Cellular Longevity* 2022**,** 7494863. doi: 10.1155/2022/7494863.

Jiang, X., Liu, J., Lin, Q., Mao, K., Tian, F., Jing, C., et al. (2017). Proanthocyanidin prevents lipopolysaccharide-induced depressive-like behavior in mice via neuroinflammatory pathway. *Brain Research Bulletin* 135**,** 40-46. doi: 10.1016/j.brainresbull.2017.09.010.

Kurinami, H., Shimamura, M., Ma, T., Qian, L., Koizumi, K., Park, L., et al. (2014). Prohibitin viral gene transfer protects hippocampal CA1 neurons from ischemia and ameliorates postischemic hippocampal dysfunction. *Stroke* 45(4)**,** 1131-1138. doi: 10.1161/STROKEAHA.113.003577.

Lachen-Montes, M., Gonzalez-Morales, A., Zelaya, M.V., Perez-Valderrama, E., Ausin, K., Ferrer, I., et al. (2017). Olfactory bulb neuroproteomics reveals a chronological perturbation of survival routes and a disruption of prohibitin complex during Alzheimer's disease progression. *Sci Rep* 7(1)**,** 9115. doi: 10.1038/s41598-017-09481-x.

Lachén-Montes, M., González-Morales, A., Zelaya, M.V., Pérez-Valderrama, E., Ausín, K., Ferrer, I., et al. (2017). Olfactory bulb neuroproteomics reveals a chronological perturbation of survival routes and a disruption of prohibitin complex during Alzheimer's disease progression. *Scientific Reports* 7(1)**,** 9115. doi: 10.1038/s41598-017-09481-x.

Li, N., Worthmann, H., Deb, M., Chen, S., and Weissenborn, K. (2011). Nitric oxide (NO) and

asymmetric dimethylarginine (ADMA): their pathophysiological role and involvement in intracerebral hemorrhage. *Neurological Research* 33(5)**,** 541-548. doi: 10.1179/016164111X13007856084403.

Li, P., Tang, T., Liu, T., Zhou, J., Cui, H., He, Z., et al. (2019). Systematic Analysis of tRNA-Derived Small RNAs Reveals Novel Potential Therapeutic Targets of Traditional Chinese Medicine (Buyang-Huanwu-Decoction) on Intracerebral Hemorrhage. *International Journal of Biological Sciences* 15(4)**,** 895-908. doi: 10.7150/ijbs.29744.

Luo, J., Zeng, K., Zhang, C., Fang, M., Zhang, X., Zhu, Q., et al. (2012). Down-regulation of CRMP-1 in patients with epilepsy and a rat model. *Neurochemical Research* 37(7)**,** 1381-1391. doi: 10.1007/s11064-012-0712-6.

MacArthur, I.C., Bei, Y., Garcia, H.D., Ortiz, M.V., Toedling, J., Klironomos, F., et al. (2019). Prohibitin promotes de-differentiation and is a potential therapeutic target in neuroblastoma. *JCI Insight* 5. doi: 10.1172/jci.insight.127130.

Osman, C., Merkwirth, C., and Langer, T. (2009). Prohibitins and the functional compartmentalization of mitochondrial membranes. *Journal of Cell Science* 122(Pt 21)**,** 3823-3830. doi: 10.1242/jcs.037655.

Pan, C., Liu, N., Zhang, P., Wu, Q., Deng, H., Xu, F., et al. (2018). EGb761 Ameliorates Neuronal Apoptosis and Promotes Angiogenesis in Experimental Intracerebral Hemorrhage via RSK1/GSK3β Pathway. *Molecular Neurobiology* 55(2)**,** 1556-1567. doi: 10.1007/s12035-016-0363-8.

Qu, Y., Konrad, C., Anderson, C., Qian, L., Yin, T., Manfredi, G., et al. (2020). Prohibitin S-Nitrosylation Is Required for the Neuroprotective Effect of Nitric Oxide in Neuronal Cultures. *The Journal of Neuroscience : the Official Journal of the Society For Neuroscience* 40(16)**,** 3142-3151. doi: 10.1523/JNEUROSCI.1804-19.2020.

Sawyer, R.P., Yim, E., Coleman, E., Demel, S.L., Sekar, P., and Woo, D. (2021). Impact of Preexisting Cognitive Impairment and Race/Ethnicity on Functional Outcomes Following Intracerebral Hemorrhage. *Stroke* 52(2)**,** 603-610. doi: 10.1161/STROKEAHA.120.030084.

Schrag, M., and Kirshner, H. (2020). Management of Intracerebral Hemorrhage: JACC Focus Seminar. *Journal of the American College of Cardiology* 75(15)**,** 1819-1831. doi: 10.1016/j.jacc.2019.10.066.

Tao, W., Lee, J., Chen, X., Díaz-Alonso, J., Zhou, J., Pleasure, S., et al. (2021). Synaptic memory requires CaMKII. *ELife* 10. doi: 10.7554/eLife.60360.

Wei, J., Dai, S., Pu, C., Luo, P., Yang, Y., Jiang, X., et al. (2022). Protective role of TLR9-induced macrophage/microglia phagocytosis after experimental intracerebral hemorrhage in mice. *CNS Neurosci Ther*. doi: 10.1111/cns.13919.

Wu, Y., Wang, L., Hu, K., Yu, C., Zhu, Y., Zhang, S., et al. (2018). Mechanisms and Therapeutic Targets of Depression After Intracerebral Hemorrhage. *Frontiers In Psychiatry* 9**,** 682. doi: 10.3389/fpsyt.2018.00682.

Xue, M., and Yong, V.W. (2020). Neuroinflammation in intracerebral haemorrhage: immunotherapies with potential for translation. *The Lancet. Neurology* 19(12)**,** 1023-1032. doi: 10.1016/S1474-4422(20)30364-1.

Yan, C., Gong, L., Chen, L., Xu, M., Abou-Hamdan, H., Tang, M., et al. (2020). PHB2 (prohibitin 2) promotes PINK1-PRKN/Parkin-dependent mitophagy by the PARL-PGAM5-PINK1 axis. *Autophagy* 16(3)**,** 419-434. doi: 10.1080/15548627.2019.1628520.

Yang, Y., Zhang, M., Kang, X., Jiang, C., Zhang, H., Wang, P., et al. (2015). Thrombin-induced microglial activation impairs hippocampal neurogenesis and spatial memory ability in mice. *Behavioral and Brain Functions : BBF* 11(1)**,** 30. doi: 10.1186/s12993-015-0075-7.

Zanca, R.M., Sanay, S., Avila, J.A., Rodriguez, E., Shair, H.N., and Serrano, P.A. (2019). Contextual fear memory modulates PSD95 phosphorylation, AMPAr subunits, PKMζ and PI3K differentially between adult and juvenile rats. *Neurobiology of Stress* 10**,** 100139. doi: 10.1016/j.ynstr.2018.11.002.

Zhang, T., Zhang, Y., Cui, M., Jin, L., Wang, Y., Lv, F., et al. (2016). CaMKII is a RIP3 substrate mediating ischemia- and oxidative stress-induced myocardial necroptosis. *Nature Medicine* 22(2)**,** 175-182. doi: 10.1038/nm.4017.

Zhou, P., Qian, L., D'Aurelio, M., Cho, S., Wang, G., Manfredi, G., et al. (2012). Prohibitin reduces mitochondrial free radical production and protects brain cells from different injury modalities. *The Journal of Neuroscience : the Official Journal of the Society For Neuroscience* 32(2)**,** 583-592. doi: 10.1523/JNEUROSCI.2849-11.2012.

Figure description

Fig.1 The flow chart of experiment design.

Fig.2 PHB overexpression alleviates brain injury and neurological function of mice following ICH.
(A) The schematic diagram of intracerebral injection. (B) Images of the brain slices following collagenase injection. (C) Quantification of hematoma volumes in three groups of mice. (D) The mNSS scoring system for neural behavior. (E) The percentage of brain water content. (F) Corner test, to detect behavioral changes after brain hemorrhage. (G) Forelimb placement test, to detect the level of limb paralysis in mice after brain hemorrhage. (H) Images of Nissl staining and TUNEL staining in the hippocampal region following collagenase injection. Scale bar, 500μm for Nissl staining and 100μm for TUNEL staining. (I) Bar chart of Nissl staining positive cells. (J) Bar chart of TUNEL staining positive cells. Data are represented as mean ± SD (n=9 per group). (**p<0.01 versus the sham group, ***p<0.001 versus the sham group, $^{\#}$p< 0.05 versus the ICH group, $^{\#\#}$p<0.01 versus the ICH group,$^{\#\#\#}$p<0.001 versus the ICH group)

Fig.3 Changes in cerebral blood flow after PHB overexpression.
(A) Images of cerebral blood flow in mice in different groups. (B) Images of brain areas with cerebral blood flow values. (C) Line chart of the comparison of cerebral blood flow values. Data are represented as mean ± SD (n=9 per group). (*p<0.05 versus the sham group, $^{\#}$p<0.05 versus the ICH group)

Fig.4 PHB overexpression significantly inhibits inflammation and ferroptosis in ICH mice.
(A) Images of Perls staining and IHC of GFAP, Iba-1, and IL-1β-positive neuronal cells in the perihematomal area of mice in different groups. (B-E) Representative bar charts of Perls staining and expression of GFAP, Iba-1, and IL-1β-positive neuronal cells in IHC. Data are represented as mean ± SD (n=4 per group). (***p<0.001 versus the sham group, $^{\#\#}$p<0.01 versus the ICH group)

Fig.5 PHB can effectively alleviate memory loss and depression-like symptoms in mice after ICH.
(A) The time flow of behavioral tests assessing learning, memory, and depression-like symptoms. (B, C) Trajectory and Images of Morris water maze to detect memory function in mice. (D) Bar charts of Y-maze test, which detect spatial memory in mice. (E) Images of Rotarod Test assessing mice memory ability. (F) Social test images reflect social function in mice. (F) Startle test graphs show the impairment of scene memory ability in mice. (G) Nest building test line graphs showing the degree of autism in mice. Data are expressed as mean ± SD (n=9 per group). (ns, no significant difference, **p<0.01 versus the sham group, ***p<0.001 versus the sham group, $^{\#}$p< 0.05 versus the ICH group, $^{\#\#}$p<0.01 versus the ICH group,$^{\#\#\#}$p<0.001 versus the ICH group) Abbreviations: RT=Rotarod Test; ST-1=Startle Test; NBT=Nest Building Test; YMT=Y-maze Test; MWM= Morris Water Maze; ST-2=Social Test.

Fig.6 PHB alleviates depression-like symptoms in ICH mice.
(A) The timeline of depression-like behavioral assessments. (B) Bar chart of sucrose preference test. (C, D) Graphs of forced swimming test in total immobility time of mice. (E, F) Figures of tail suspension test in total immobility time of mice. Data are represented as mean ± SD (n=8 per group). (**p<0.01 versus the sham group, ***p<0.001 versus the sham group, $^{\#}$p<0.05 versus the

ICH group) Abbreviations: FST=Forced Swimming Test; TST=Tail Suspension Test; SPT= Sucrose Preference Test.

Fig.7 PHB improves learning, memory, and cognitive impairment in ICH mice
(A) Heatmap analysis showing 31 detected genes involved in PHB expression. (n=2 per group, each sample pooled from 3 mice) (B) Analysis of the mechanisms of action involved in PHB. (C) Gene sequencing analysis of the most relevant mechanisms of action (D) Calcium channel enrichment analysis generated from the GSEA analysis (E) CAMP pathway enrichment analysis generated from the GSEA analysis (F) LTP enrichment analysis generated from the GSEA analysis (G) serotonergic synapse enrichment analysis generated from the GSEA analysis (H) axon guidance enrichment analysis generated from the GSEA analysis (I) Representative western blotting of PSD-95, NLGL-1, BDNF, CAMK-2 and CRMP-1 in mice exposed to collagenase injection. (J) Immunofluorescence staining graphs showing SYP positive level. Data are expressed as mean ± SD (n=6 per group). ($^{***}p<0.001$ versus the sham group, $^{\#\#}p<0.01$ versus the ICH group,$^{\#\#\#}p<0.001$ versus the ICH group)

Figure 1.TIF

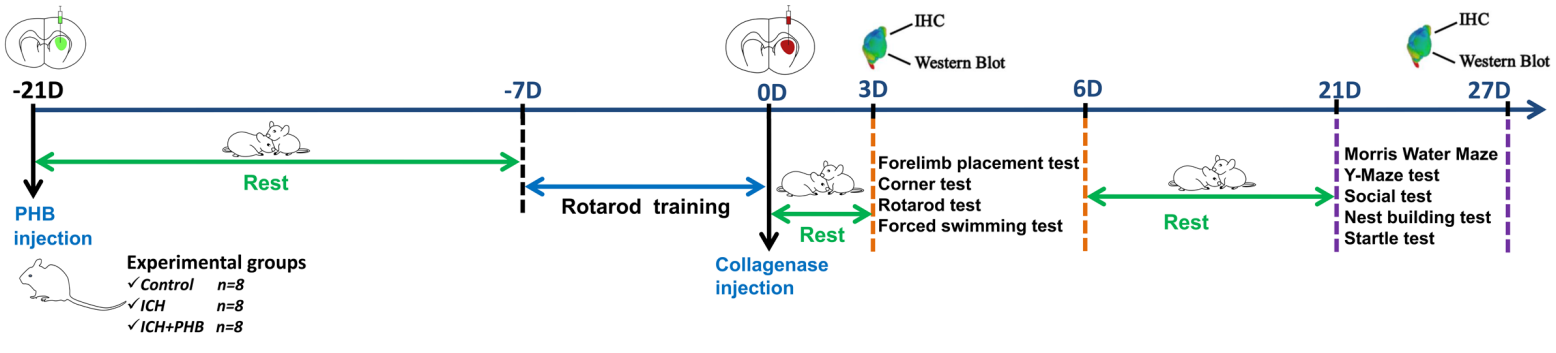

Figure 2.TIF

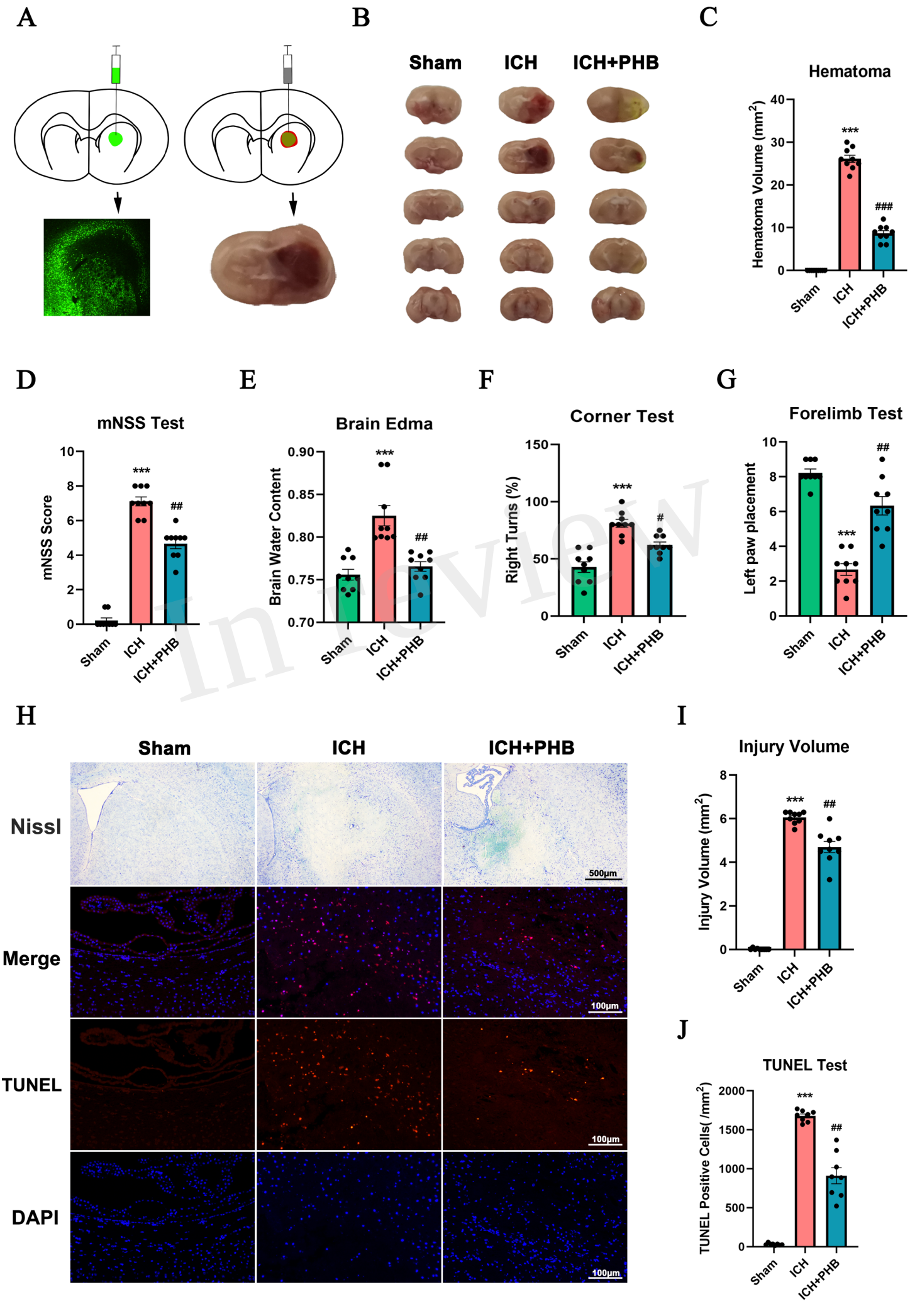
A
B
C
Sham
ICH
ICH+PHB
Hematoma
Hematoma Volume (mm2)
D
mNSS Test
mNSS Score
E
Brain Edma
Brain Water Content
F
Corner Test
Right Turns (%)
G
Forelimb Test
Left paw placement
H
Nissl
Merge
TUNEL
DAPI
500μm
100μm
I
Injury Volume
Injury Volume (mm2)
J
TUNEL Test
TUNEL Positive Cells(/mm2)

Figure 3.TIF

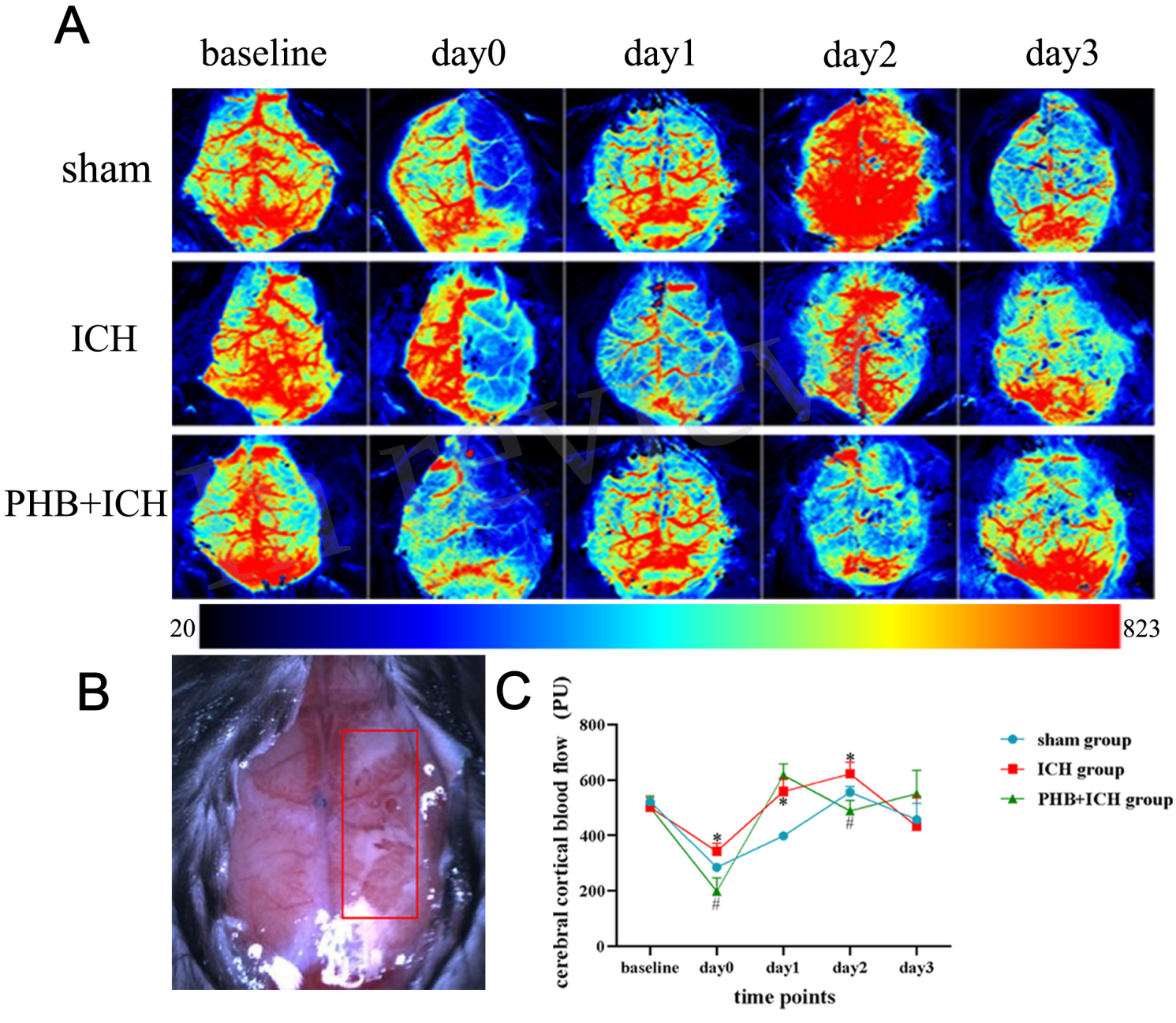
A
baseline
day0
day1
day2
day3
sham
ICH
PHB+ICH
20
823
B
C
cerebral cortical blood flow (PU)
800
600
400
200
0
baseline
day0
day1
day2
day3
time points
sham group
ICH group
PHB+ICH group

Figure 4.TIF

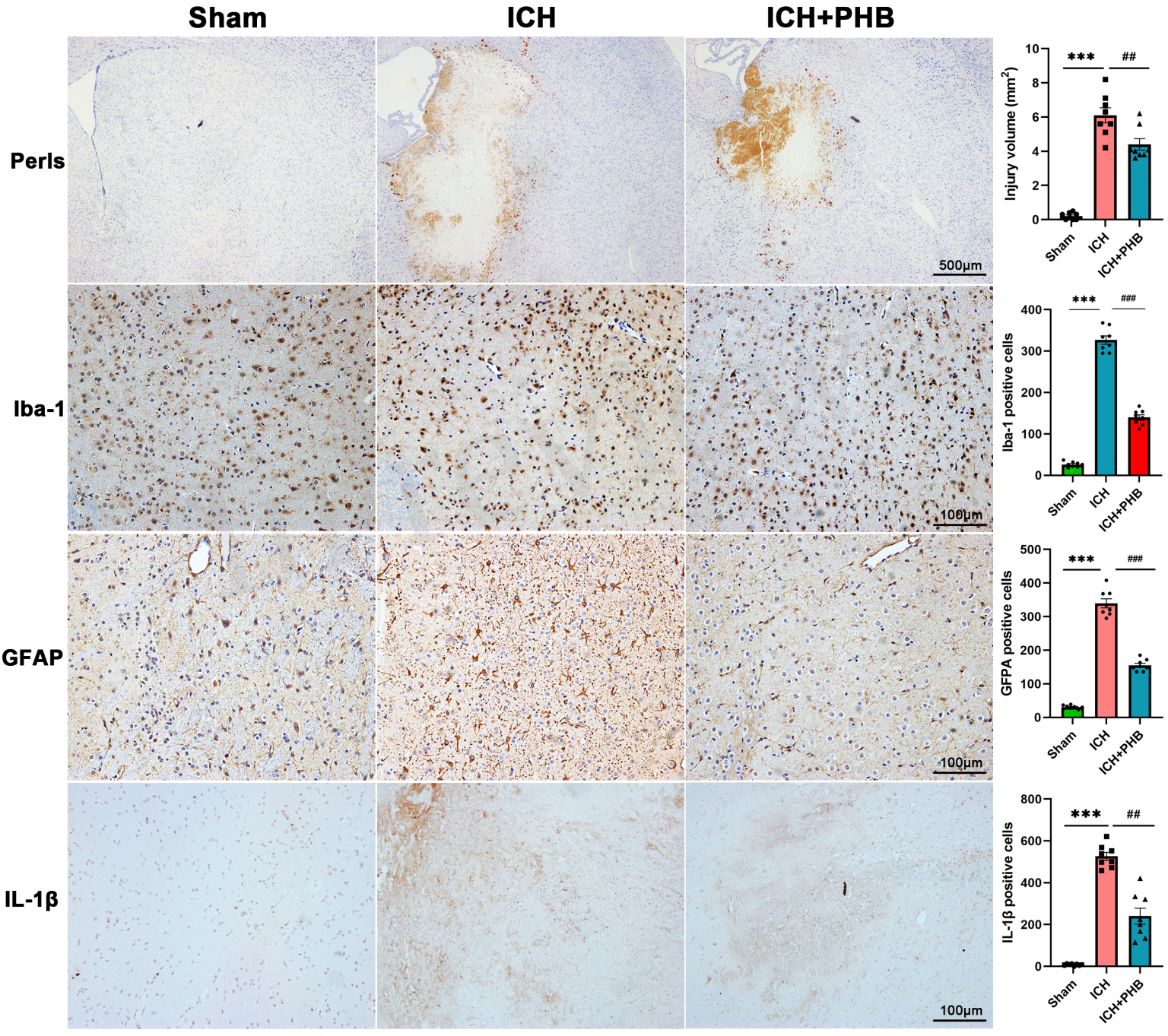
Sham
ICH
ICH+PHB
Perls
Iba-1
GFAP
IL-1β
500μm
100μm
100μm
100μm
Injury volume (mm²)
Iba-1 positive cells
GFPA positive cells
IL-1β positive cells
***
##
###
Sham
ICH
ICH+PHB

Figure 5.TIF

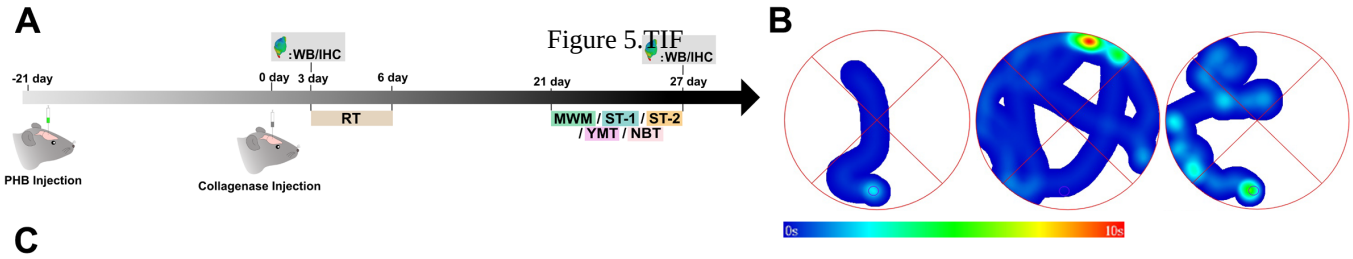

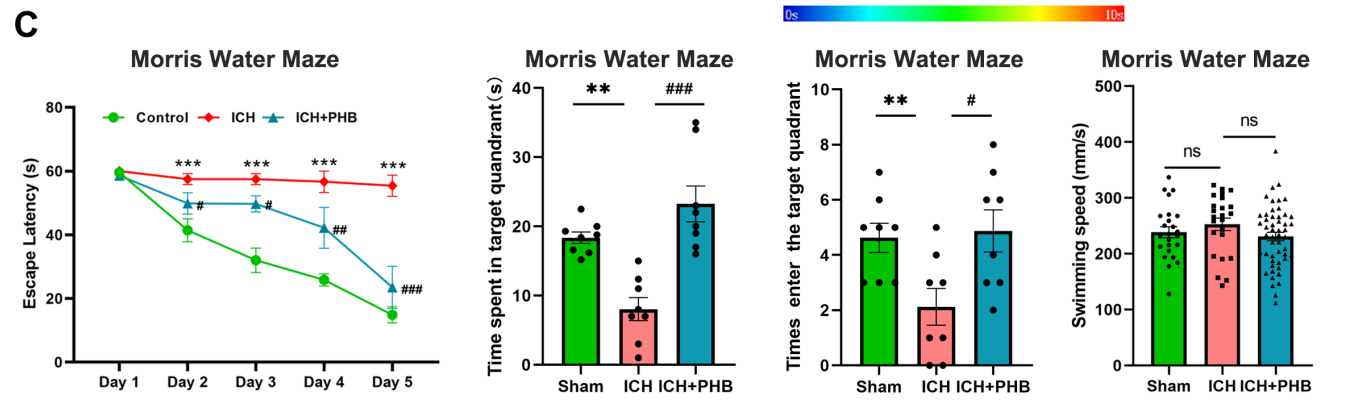

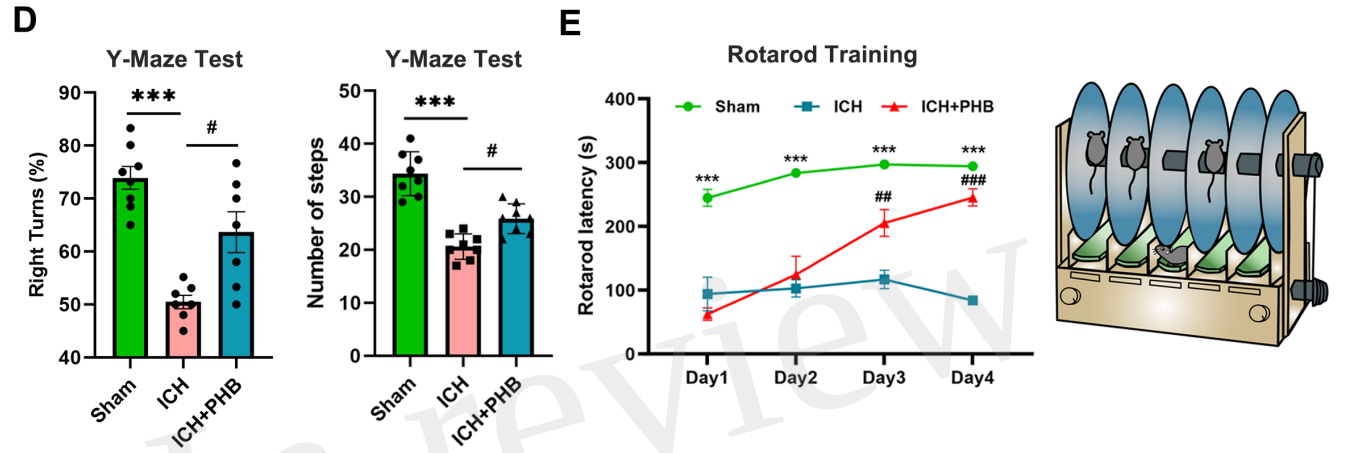

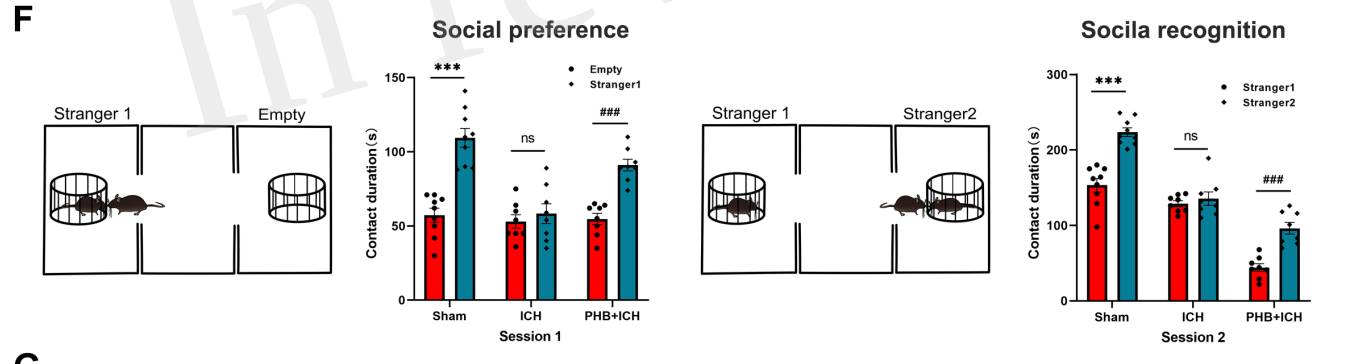

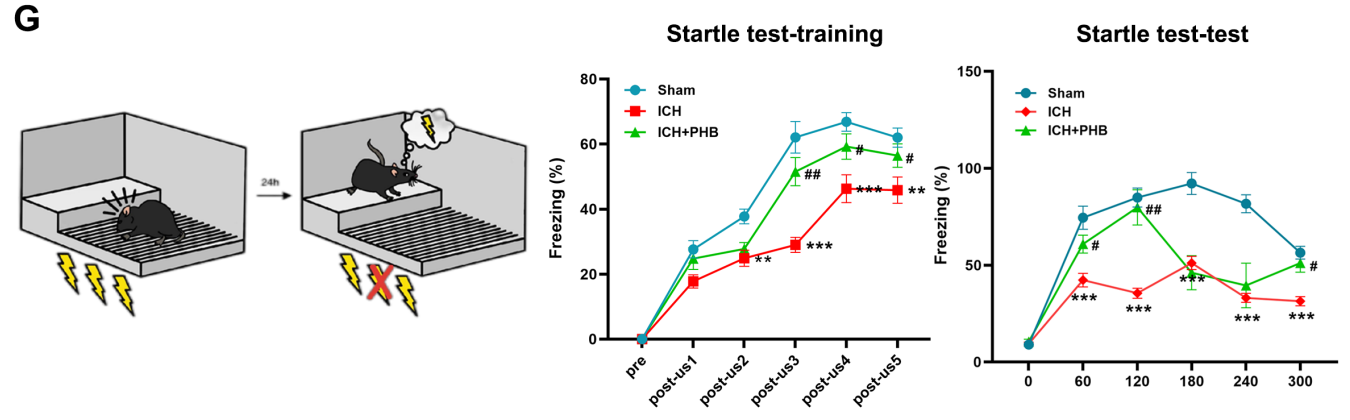

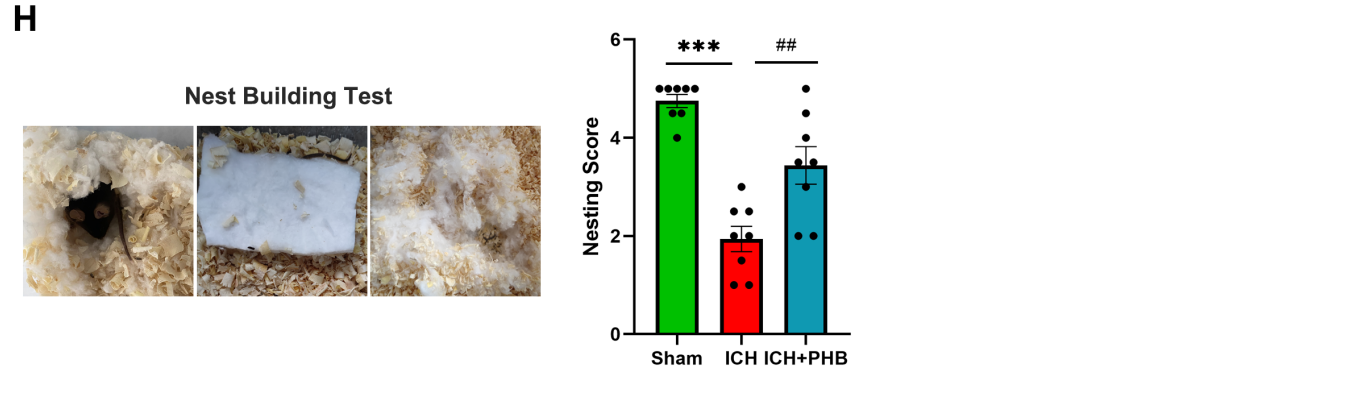

Figure 6.TIF

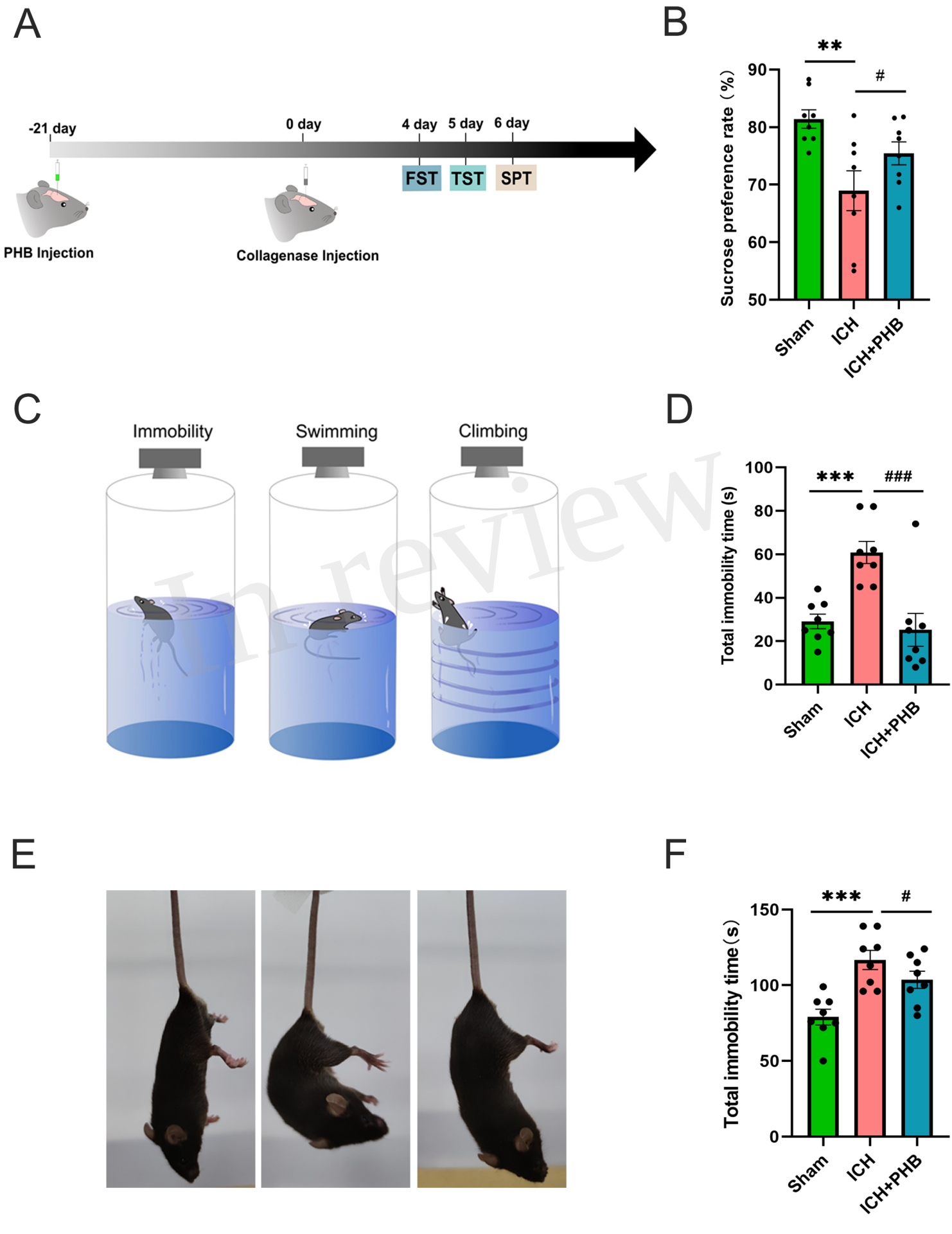

Figure 7.JPEG